Position-Dependent Local Detection Efficiency in a Nanowire Superconducting Single-Photon Detector

J.J. Renema,* Q. Wang, I. Komen, M.P. van Exter, and M.J.A. de Dood
Leiden Institute of Physics, Leiden University, Niels Bohrweg 2, 2333 CA Leiden, the Netherlands

R. Gaudio, K. op 't Hoog, D. Sahin, and A. Fiore
COBRA Research Institute, Eindhoven University of Technology, P.O. Box 513, 5600 MB Eindhoven, The Netherlands

A. Schilling and A. Engel
Physics Institute of the University of Zurich, Winterthurerstr. 190, 8057 Zurich, Switzerland

arXiv:1504.05003v1 [cond-mat.supr-con] 20 Apr 2015

We probe the local detection efficiency in a nanowire superconducting single-photon detector along the cross-section of the wire with a spatial resolution of 10 nm. We experimentally find a strong variation in the local detection efficiency of the device. We demonstrate that this effect explains previously observed variations in NbN detector efficiency as function of device geometry.

Nanowire superconducting single-photon detectors (SSPDs) consist of a superconducting wire of nanoscale cross-section [1], typically 4 nm by 100 nm. Photon detection occurs when a single quantum of light is absorbed and triggers a transition from the superconducting to the normal state. SSPDs have high efficiency, low jitter, low dark count rate and fast reset time [2], and are therefore a key technology for, among others, quantum key distribution [3], interplanetary communication [4] and cancer research [5].

Although progress has been made recently, the underlying physical mechanism responsible for photon detection on the nanoscale is still under active investigation. A combination of theory [6, 7], experiments [8–10] and simulations [11, 12] on NbN SSPDs indicates that the absorption of a photon destroys Cooper pairs in the superconductor and creates a localized cloud of quasiparticles that diverts current across the wire. This makes the wire susceptible to the entry of a superconducting vortex from the edge of the wire. Energy dissipation by this moving vortex drives the system to the normal state.

An important and unexpected implication of this detection model is a nanoscale position variation in the photodetection properties of the device. The conditions at the entry point of the vortex determine the energy required for it to cross the wire. This causes photons absorbed close to the edge to have a local detection efficiency (LDE) [13] compared to photons absorbed in the center of the wire [12]. This effect has practical implications for the operation of SSPDs, since it represents a potential limitation of the detection efficiency. In addition, SSPDs have been proposed for nanoscale sensing, either in a near-field optical microscope configuration [14] or as a subwavelength multiphoton probe [15], where this effect would be of major importance for the properties of such a microscope. While this effect has been predicted theoretically, clear experimental evidence is missing.

* renema@physics.leidenuniv.nl

In this work, we experimentally explore the nanoscale variations in the intrinsic response of the detector. We spatially resolve the LDE with a resolution of approximately 10 nm, better than $\lambda/50$, using far-field illumination only. We find that our results are qualitatively consistent with numerical simulations [11, 12]. Our results provide excellent quantitative agreement with experiments that indicate a polarization dependence in the LDE that was hitherto not understood [16].

The key technique used in this work is a differential polarization measurement that probes the IDE of the detector (see Figure 1). The technique is based on the fact that polarized light is absorbed preferentially in different positions for the two orthogonal polarizations, due to differences in boundary conditions. Using this technique, we achieve selective illumination of either the sides or the middle of the wire, which we use to probe the intrinsic photodetection properties of our device on the nanoscale.

However, it is well known that changing the polarization results in a change in overall optical absorption probability [16–20]. In order to correct for this effect, we must separate the probability that a photon is absorbed from the probability that an absorbed photon causes a detection event. To separate changes in optical absorption from the intrinsic LDE effects which are presently of interest, we use quantum detector tomography (QDT) [8, 9, 21–29].

QDT records the detector response to a set of known quantum states of light and distills from these measurements the detection probability for different photon numbers. As we showed previously [28], this procedure allows us to unambiguously separate the intrinisic one-photon detection probability p_1 from the probability η that a photon is absorbed [30]. We found that η is almost independent of detector bias current and that the value is consistent with the geometric area of the detector. Hence, we identify p_1 with the detection probability conditional on photon absorption, which we dub the internal detection efficiency (IDE). By construction, $\mathrm{IDE} = \int \mathrm{LDE}(x)A(x)dx / \int A(x)dx$, where the integral

runs along the cross-section of the wire and $A(x)$ represents the absorption probability density.

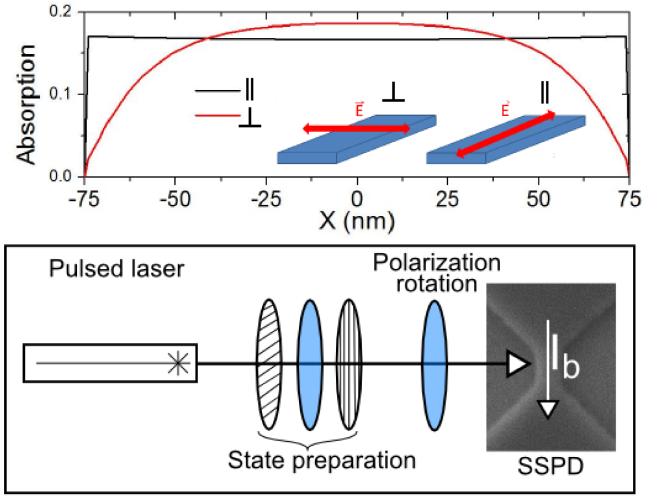

Figure 1. Sketch of our experiment. *Top:* Absorption as a function of position in the wire for parallel (∥) and perpendicular (⊥) polarizations, calculated with an FDTD method (see text). *Inset*: Sketch showing the two polarizations. The red arrow represents the polarization of the electric field. *Bottom*: Experimental setup. Our laser pulses are tuned in intensity by a variable attenuator consisting of two crossed polarizers and a $\lambda/2$ wave plate. Polarization is set by an additional $\lambda/2$ wave plate. The image is a SEM micrograph of a detector nominally identical to the one used in this experiment.

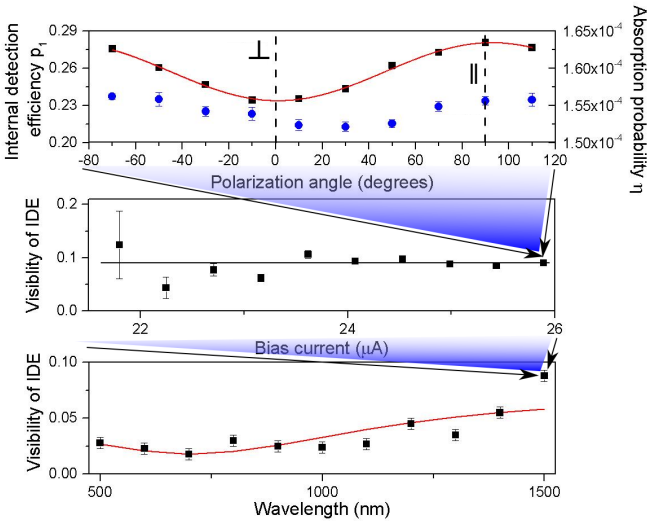

Figure 2. Experimental results on the polarization dependence of the internal detection efficiency (IDE). Each graph represents one data point in the graph below it. *Top panel, black squares:* IDE as a function of polarization at an excitation wavelength of 1500 nm at $I_b = 25.8$ μA. The red line is a sine fit. *Top panel, blue circles:* Absorption probability as a function of polarization. *Middle panel:* IDE as a function of bias current. We find that the IDE is independent of bias current. The black line represents the weighted average of our measurements at different bias currents. *Bottom panel:* IDE as a function of illumination wavelength. We show the fit of the observed polarization-dependent IDE to the position-dependent local detection efficiency (LDE).

We perform our experiments on a 100 nm long, 150 nm wide NbN bridge patterned from a 5 nm-thick NbN film sputtered on a GaAs substrate [31] ($I_c = 28$ μA). We apply a bias current and read out the detector with a bias-tee to separate high-frequency detection pulses from the DC bias current. The resulting pulses are fed to a series of RF amplifiers and a pulse counter. At each combination of bias current, photon energy and polarization, we record the detector count rate as a function of input intensity. The probe states were prepared by a broadband pulsed laser (Fianium, repetition rate 20 MHz) out of which we select a narrow wavelength band with dielectric filters [9]. We prepare the desired intensity and polarization by first attenuating the light with a combination of two crossed polarizers and a half-wave plate, and then setting the polarization with an additional wave plate (see Figure 1) [32].

Figure 2 shows our measured IDE and η, as function of polarization and wavelength. The top panel shows the IDE of our device as a function of the polarization of light with $\lambda = 1500$ nm wavelength. Our experiments show that the IDE and absorption probability oscillate in phase when the polarization is rotated, with a minimum at perpendicular polarization and a maximum at parallel polarization. This demonstrates that absorption of TM-polarized photons is less likely to result in a detection. This polarization is absorbed preferentially in the middle of the wire. Our result therefore confirms earlier, preliminary results [16, 33, 34] that suggested that the edges of the detector are more efficiently photodetecting than the center of the wire. The error bars in this panel correspond to the standard deviation of a series of independent experiments. The middle panel of Figure 2 shows that the visibility of the IDE $V_{IDE} = (p_{max} - p_{min})/(p_{max} + p_{min})$ is independent of bias current. We can therefore associate one visibility to a particular illumination wavelength. For $\lambda = 1500$ nm we find $V_{IDE} = 0.09$. The bottom panel shows the wavelength dependence of the visibility. We find that longer wavelengths have higher visibility in the IDE. In this panel, we show a fit to our position-dependent LDE, which we will discuss below.

In the second part of this work, we will discuss our reconstruction of the LDE profile from these measurements. We make use of the fact that the IDE is given by the LDE multiplied by the optical absorption probability, integrated across the wire. Our strategy is to take the absorption profiles as given - since they are well studied - and to take the LDE profile as a free parameter and fit it to our experimental data.

To calculate the optical absorption distributions, we perform a series of numerical simulations at different wavelengths using a finite-difference time domain (FDTD) method (RSOFT Fullwave). We perform a 2D

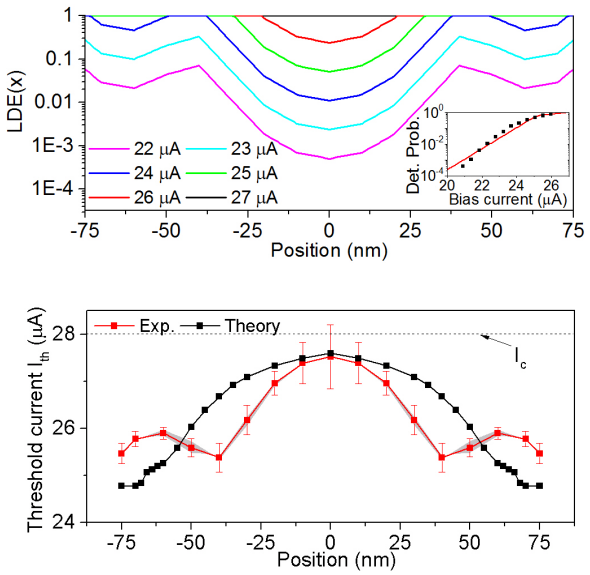

Figure 3. Local detection efficiency (LDE) and threshold current in an SSPD, for $\lambda = 1500$ nm. *Top panel*: observed positional variations in the LDE of an SSPD, as a function of bias current. *Inset*: IDE, as a function of bias current. *Bottom panel:* Threshold current I_{th}. The red curve shows the experimentally observed value, the black curve shows the theoretical value obtained from numerical modelling of the detection event.

simulation, and compute the electric field in a 150 nm wide, 5 nm thick NbN wire on a semi-infinite GaAs substrate and an 80 nm thick HSQ layer on top of the NbN wire. The refractive index of NbN deposited film on GaAs is derived from spectroscopic ellipsometry measurements [35] [36]. In Figure 1, the result of this calculation is shown for $\lambda = 1500$ nm.

In order to combine information from different wavelengths - which is required to find the LDE - we must posit some relation between photon energy and detection probability [37]. Our ansatz is motivated by the experimental observation that for low detection probabilities, the detection probability depends exponentially on bias current, by our earlier work on the energy-current relation in SSPDs, and on the numerical simulations described below [8, 9, 11, 12]. We model the bias current dependence of the LDE as $\mathrm{LDE}(x) = \min\{1, \exp(I_b - I_{th}(x))/I^\star\}$, with $I_{th}(x) = I_c - \gamma'(x)E$, where I_b is the applied bias current, I_c is the critical current, E is the photon energy, and $I^\star = 0.65$ μA is an experimentally determined current scale. $\gamma'(x)$ is the local energy-current interchange ratio, which parametrizes the detection probability of the wire at different excitation wavelengths. These simple, empirical expressions enable us to combine our wavelength- and, polarization-dependent IDE measurements, and compute the LDE.

The top panel of Figure 3 shows the resulting LDE profile for different bias currents, for a wavelength of 1500 nm. We obtained this result by fitting $\gamma'(x)$ to the experimentally determined visibility of the polarization-dependent IDE in the range $\lambda = 500 - 1500$ nm, using the calculated absorption profiles. We find that the LDE has a high value at the edges of the wire, up to a point roughly 40 nm from the edge. From there, the detection efficiency decreases; it is reduced by two orders of magnitude at the center of the wire. The LDE is current-dependent, but saturation sets in around $I_b = 25.5$ μA ($I_b/I_c = 0.91$).

The inset in the top panel of Figure 3 shows the effect of this saturation on the IDE. There are three regimes: a rolloff regime, where the detection property depends exponentially on bias current, a plateau regime at high currents, where LDE = 1, implying IDE = 1, and an intermediate regime of slowly increasing detection probability. These regimes are marked by dashed lines in the inset. In the middle regime, parts of the detector are fully photodetecting, while other parts are still in a fluctuation-assisted regime [38]. The variations between the experimental data and the values calculated from our fit are less than a factor of 2, which demonstrates the self-consistency of our results. We have also confirmed that the observed LDE profile reproduces the fact (see Figure 2, middle panel) that in our measurement range, the visibility of the polarization-dependent IDE does not depend on the applied bias current. From these observations, we conclude that our description is able to explain all of the available experimental data regarding polarization and bias current dependence of the photoresponse of this detector.

We estimate the resolution in our measurement by varying the distance Δx at which we specify $\gamma'(x)$. In particular, we find that for $\Delta x \approx w/2$, we are unable to explain our experimentally observed data. Therefore, we conclude that the LDE profile varies with a length scale smaller than the dimensions of the wire. We find that we achieve the best fit at $\Delta x = 10$ nm. From this, we conclude that this is the resolution of our experiment.

The bottom panel of Figure 3 shows the threshold current $I_{th}(x)$. The red curve shows the experimental value, from which the LDE(x) shown in the top panel is derived. The black curve in the bottom panel of Figure 3 shows an independent, ab initio calculation of the threshold current based on the model described below. This ab initio calculation of the position-dependent detection probability is based on a numerical model [11, 12] that determines the threshold current for the detection of an absorbed photon of a given wavelength using a combination of quasiparticle diffusion, current displacement and vortex entry [39]. We find reasonable agreement between our observed experimental results and the theoretical values. From this, we conclude that this model captures the essential physics of the detection process in SSPDs.

Our ab initio calculation gives a physical explanation for the enhanced efficiency at the edges of the wire in terms of our microscopic model. Comparing a photon absorption in the center of the wire to one at the edge, there are two differences. First, for an absorption event

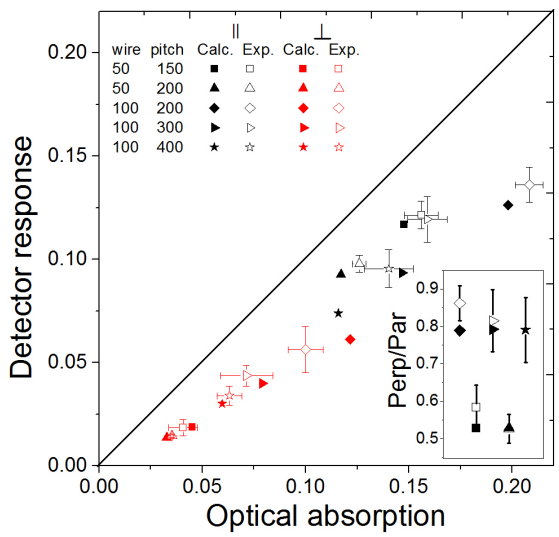

Figure 4. Internal detection efficiency (IDE) of a set of SSPD meander devices. The solid symbols represent our calculation, and the open symbols represent experimental data from [16]. Red symbols represent perpendicular ($\perp$) polarization, and black symbols represent parallel ($\parallel$) polarization. The shape of the symbol represents the wire and pitch of the detector (see legend). The error bars on the experimental data represent the spread in properties between detectors of the same design. The diagonal line represents the case IDE = 1. *Inset* Ratio of overall absorption for the two polarizations.

at the edge, the current density at the edge of the wire is reduced, due to the reduction in the number of superconducting electrons n_s. However, this is more than compensated by the reduction of the vortex self-energy, which is proportional to n_s. Vortices enter more easily when the superconductivity is weakened at their entry point, and that makes the detector more efficient at the edges.

We note that there is some disagreement in theoretical literature about the predicted shape of the LDE curve. The alternative model of Zotova *et al.* [40], which is based on the Ginzburg-Landau formalism, naturally takes into account vortex entry. However, it disregards quasiparticle diffusion and implements a hotspot with hard boundaries. The results from this model disagree strongly with our experimental results: there, a W-shaped threshold current profile is predicted, with threshold currents at the edges almost as high as in the center of the wire. The discrepancy between the models occurs precisely at the point where their 'hard' hotspot touches the edge of the wire. We speculate that both models, if refined more, will likely converge.

In the final part of this work, we discuss the implication of these results to the construction and operation of SSPD devices. In the work of Anant *et al.* [16], the IDE of a series of meander SSPDs of different wire width and pitch (wire separation) was measured. Using similar methods as described above, we compute the position-dependent optical absorption of such structures for the film properties given in that work. We use the observed LDE curve from our experiment, and compute the IDE and overall detection probability of such devices, using the same expressions which we used for our sample to obtain the LDE from the IDE and the optical absorption [41].

Figure 4 shows that this prediction agrees with the data. The calculation confirms the general claim made by Anant *et al.* that parallel polarization has a higher IDE than perpendicular. Beyond that, we are also able to compute the IDE for each device independently. The inset of Figure 4 shows the ratio of the overall efficiency for the two polarizations, which factors out the optical absorption as well as - to first order - the effect of bias current. It is therefore the most direct test of our IDE. We find excellent agreement. This demonstrates that we have achieved quantitative understanding of the internal properties of an SSPD. It also demonstrates that our results are neither limited to the SSPD on which we performed our experiment nor by our single-wire geometry.

To obtain a nonunity IDE, we must assume that the highly efficient detectors reported in [16] were not biased to their critical current. It is well known that the presence of current crowding in the bends of a wire can cause reduction of the device critical current by as much as 40% [42], with typical values of 10-20% [43]. We have assumed $I_b/I_c \approx 0.9$ for all devices to produce Figure 4. This demonstrates that our results are relevant for the kind of SSPDs which are used for applications, at the typical currents at which they are operated. It also shows that our results can be used as an all-optical method for measuring the amount of current crowding in these devices. Since the differences between the two optical absorption profiles become larger at longer wavelengths, we expect our results to be particularly relevant for the engineering of SSPDs at mid-infrared wavelengths.

In conclusion, we have demonstrated that the local detection efficiency of an SSPD depends on the position along the cross-section at which the photon is absorbed. We have probed this effect with a resolution of approximately 10 nm, and found agreement with theoretical calculations done in the context of the diffusion-based vortex crossing model. From this, we conclude that this model contains the essential features for a complete microscopic picture of the detection model in SSPDs. We have compared these predictions of our work to results reported on devices used for applications and found good agreement, demonstrating the relevance of our results for SSPD engineering. These results enable quantitative modeling of the internal properties of SSPDs.

ACKNOWLEDGMENTS

We thank D. Boltje for technical assistance, F. Schenkel for assistance with the experimental apparatus, M. Frick for assistance with programming and E.F.C. Driessen for critical reading of the manuscript. This work is part of the research programme of the Foundation for Fundamental Research on Matter (FOM), which is financially supported by the Netherlands Organisation for Scientific Research (NWO). It is also supported by NanoNextNL, a micro- and nanotechnology program of the Dutch Ministry of Economic Affairs, Agriculture and Innovation (EL&I) and 130 partners, and by the Swiss National Science Foundation grant no. 200021_146887/1. DS was supported by the Marie Curie Actions within the Seventh Framework Programme for Research of the European Commission, under the Initial Training Network PICQUE, Grant No. 608062.

[1] G. N. Goltsman, O. Okunev, G. Chulkova, A. Lipatov, A. Semenov, K. Smirnov, B. Voronov, A. Dzardanov, C. Williams, and R. Sobolewski, Appl. Phys. Lett. **79**, 705 (2001).

[2] C. Natarajan, M. Tanner, and R. Hadfield, Supercond. Sci. Technol **25**, 063001 (2012).

[3] H. Takesue, S. Nam, Q. Zhang, R. Hadfield, T. Honjo, K. Tamaki, and Y. Yamamoto, Nature Photon. **1**, 343 (2007).

[4] D. M. Boroson, J. J. Scozzafava, D. V. Murphy, and B. S. Robinson, 2009 Third IEEE International Conference on Space Mission Challenges for Information Technology , 23 (2009).

[5] N. Gemmell, A. McCarthy, B. Liu, M. Tanner, S. Dorenbos, V. Zwiller, M. Patterson, G. Buller, B. Wilson, and H. R.H., Opt. Express **21**, 5005 (2013).

[6] L. Bulaevskii, M. Graf, C. Batista, and V. Kogan, Phys. Rev. B **83**, 144526 (2011).

[7] L. Bulaevksii, M. Graf, and V. Kogan, Phys. Rev. B **85**, 014505 (2012).

[8] J. J. Renema, G. Frucci, Z. Zhou, F. Mattioli, A. Gaggero, R. Leoni, M. J. A. de Dood, A. Fiore, and M. P. van Exter, Phys. Rev. B **87**, 174526 (2013).

[9] J. J. Renema, R. Gaudio, Q. Wang, Z. Zhou, A. Gaggero, F. Mattioli, R. Leoni, D. Sahin, M. J. A. de Dood, A. Fiore, and M. P. van Exter, Phys. Rev. Lett. **112**, 117604 (2014).

[10] R. Lusche, A. Semenov, K. Il'in, M. Siegel, Y. Korneeva, A. Trifonov, A. Korneev, G. Goltsman, D. Vodolazov, and H.-W. Hübers, J. Appl. Phys. **116**, 043906 (2014).

[11] A. Engel and A. Schilling, J. Appl. Phys. **114**, 214501 (2013).

[12] A. Engel, J. Lonsky, X. Zhang, and A. Schilling, IEEE Trans. Appl. Supercond. **25**, 2200407 (2015).

[13] We define the LDE as the conditional probabilty of a detection event, given photoabsorption at a particular location.

[14] Q. Wang and M. J. de Dood, Opt. Express **21**, 3682 (2013).

[15] D. Bitauld, F. Marsili, A. Gaggero, F. Mattioli, R. Leoni, S. Jahanmirinejad, F. Lévy, and A. Fiore, Nano Lett. **10**, 2977 (2010).

[16] V. Anant, A. J. Kerman, E. A. Dauler, J. Yang, K. M. Rosfjord, and K. K. Berggren, Opt. Express **16**, 10750 (2008).

[17] E. F. C. Driessen, F. Braakman, E. Reiger, S. Dorenbos, V. Zwiller, and M. J. A. de Dood, Eur. Phys. J. Appl. Phys. **47**, 10701 (2009).

[18] E. Driessen and M. de Dood, Appl. Phys. Lett. **94**, 171109 (2009).

[19] V. Verma, F. Marsili, S. Harrington, A. Lita, R. Mirin, and S. Nam, Appl. Phys. Lett. **101**, 251114 (2012).

[20] T. Yamashita, S. Miki, H. Terai, and Z. Wang, Opt. Express **22**, 27122 (2013).

[21] J. S. Lundeen, A. Feito, H. Coldenstrodt-Ronge, K. L. Pregnell, C. Silberhorn, T. C. Ralph, J. Eisert, M. B. Plenio, and I. A. Walmsley, Nat. Phys. **5**, 27 (2008).

[22] A. Feito, J. S. Lundeen, H. Coldenstrodt-Ronge, J. Eisert, M. B. Plenio, and I. A. Walmsley, New J. Phys. **11**, 093038 (2009).

[23] M. K. Akhlaghi, A. H. Majedi, and J. S. Lundeen, Opt. Express **19**, 21305 (2011).

[24] M. K. Akhlaghi and A. H. Majedi, IEEE Trans. Appl. Supercond. **19**, 361 (2009).

[25] J. S. Lundeen, K. L. Pregnell, A. Feito, B. J. Smith, W. Mauerer, C. Silberhorn, J. Eisert, M. B. Plenio, and I. A. Walmsley, J. Mod. Optic. **56** (2009).

[26] G. Brida, L. Ciavarella, I. P. Degiovanni, M. Genovese, L. Lolli, G. Mingolla, F. Piacentini, M. Rajteri, E. Taralli, and M. G. A. Paris, New J. Phys. **14**, 085001 (2012).

[27] J. J. Renema, G. Frucci, M. J. A. de Dood, R. Gill, A. Fiore, and M. P. van Exter, Phys. Rev. A **86**, 062113 (2012).

[28] J. J. Renema, G. Frucci, Z. Zhou, F. Mattioli, A. Gaggero, R. Leoni, M. J. A. d. Dood, A. Fiore, and M. P. van Exter, Opt. Express **20**, 2806 (2012).

[29] C. Natarajan, L. Zhang, H. Coldenstrodt-Ronge, G. Donati, S. Dorenbos, V. Zwiller, I. Walmsley, and R. Hadfield, Opt. Express **21**, 893 (2013).

[30] See Supplemental material for details.

[31] A. Gaggero, S. Jahanmirinejad, F. Marsili, F. Mattioli, R. Leoni, D. Bitauld, D. Sahin, G. J. Hamhuis, R. Nötzel, R. Sanjines, and A. Fiore, Appl. Phys. Lett. **97**, 151108 (2010).

[32] While in principle it is possible to achieve the desired combination of polarizations and intensities using two independently rotating polarizers, we found that the effects of wedge in the polarizers preclude this solution.

[33] L. Maingault, P. Cavalier, R. Lamaestre, L. Frey, and J. Villegier, Proc. ASC 2008 in IEEE Trans. Appl. Supercond. (2008).

[34] D. Sahin, A. Gaggero, Z. Zhou, S. Jahanmirinejad, F. Mattioli, R. Leoni, J. Beetz, M. Lermer, M. Kamp, S. Höfling, and A. Fiore, Applied Physics Letters **103**, 111116 (2013).

[35] D. Sahin, *Waveguide Single-Photon and Photon-Number Resolving Detectors*, Ph.D. thesis, Eindhoven university

of Technology (2014).
[36] In these calculations, we neglect the effect of the tapered parts of the bridge because they have little influence on the absorption in the central, photodetecting section. See Supplemental material for details.
[37] This calculation is described in detail in the Suplemental Material.
[38] D. Y. Vodolazov, Phys. Rev. B **90**, 054515 (2014).
[39] See Supplemental material for details.
[40] A. Zotova and D. Vodolazov, Supercond. Sci. Technol. **27**, 125001 (2014).
[41] We account for the differences in width by considering the edges of our IDE profile. See Supplemental material for details.
[42] D. Henrich, P. Reichensperger, M. Hofherr, J. Meckbach, K. Il'in, M. Siegel, A. Semenov, A. Zotova, and D. Y. Vodolazov, Phys. Rev. B **86**, 144505 (2012).
[43] A. J. Kerman, E. A. Dauler, W. E. Keicher, J. K. W. Yang, K. K. Berggren, G. Goltsman, and B. Voronov, Appl. Phys. Lett. **88**, 111116 (2006).